Adaptive fuzzy terminal sliding mode control for a class of MIMO uncertain nonlinear systems

V. Nekoukar, A. Erfanian*

Neuromuscular Control Systems Laboratory, Iran Neural Technology Research Centre, Department of Biomedical Engineering, Iran University of Science and Technology (IUST), Tehran, Iran

Abstract

This paper presents a new adaptive terminal sliding mode tracking control design for a class of nonlinear systems using fuzzy logic system. The terminal sliding mode control (TSM) was developed to provide faster convergence and higher-precision control than the linear hyperplane-based sliding control. However, the original TSM encountered singularity problem with discontinuous control action. Moreover, a prior knowledge about the plant to be controlled is required. The proposed controller combines a continuous non-singular TSM with an adaptive learning algorithm and fuzzy logic system to estimate the dynamics of the controlled plant so that closed-loop stability and finite-time convergence of tracking errors can be guaranteed. The performance of the proposed control strategy is evaluated through the control of a two-link rigid robotic manipulator. Finally, the effectiveness of the proposed scheme is demonstrated through the control of the ankle and knee movements in paraplegic subjects using functional electrical stimulation. Simulation and experimental results verify that the proposed control strategy can achieve favorable control performance with regard to system parameter variations and external disturbances.
© 2011 Elsevier B.V. All rights reserved.

Keywords: Adaptive fuzzy control; Terminal sliding mode; Time-varying; Functional electrical stimulation; Fuzzy system models

1. Introduction

A useful and effective control scheme to deal with uncertainties, time varying properties, nonlinearities and bounded externals disturbances is the sliding mode control (SMC) [1,2]. The first step in the sliding mode control design is to choose a switching manifold, so that the state variables restricted to the manifold have a desired dynamics. However, conventional switching manifolds are usually linear hyperplanes which guarantee the asymptotic stability; therefore, error dynamics cannot converge to zero in finite time. The sliding mode parameters can be adjusted to get faster error convergence, however, this will, in turn, increase the control gain, which may cause severe chattering on the sliding surface and, therefore, deteriorate the system performance. To tackle the problems of globally asymptotic stabilization, terminal sliding mode (TSM) control scheme has been developed [3–5] to achieve finite-time stabilization. Different aspects of the conventional TMS control design were investigated in the literature [3–11] including singularity and chattering problems and requirement of prior knowledge about the dynamics of the process to be controlled. In order to solve the singularity problem of the initial TSM controller, several methods have been proposed. Zhihong and Yu [4]

---

* Corresponding author. Tel.: +98 21 77240465; fax: +98 21 77240490.

E-mail addresses: nekoukar@iust.ac.ir (V. Nekoukar), erfanian@iust.ac.ir (A. Erfanian).

proposed a general terminal sliding mode for MIMO linear systems and used an indirect approach to avoid singularity by switching from terminal sliding manifold to linear sliding manifold. An alternate approach proposed by Wu et al. [6] is to transfer the trajectory to a specified open region in which the terminal sliding mode control is not singular. These methods are categorized as the indirect approaches to avoid the singularity, while the method proposed by Feng et al. [7] is a direct approach to overcome the singularity problem in TSM control systems. The proposed method is a global non-singular terminal sliding mode controller for a class of nonlinear dynamical systems with parameter uncertainties and external disturbances.

All the above mentioned non-singular TSM controllers need the discontinuous control to guarantee the finite-time reachability to TSM. The chattering caused by the discontinuous control action is undesirable in many applications. To overcome this problem, Tao et al. [8] proposed a fuzzy terminal sliding mode controller for linear systems with mismatched time-varying uncertainties while the adaptive fuzzy terminal attractors have been applied and the parameters of the output fuzzy sets in the fuzzy terminal sliding mode controller were online adapted. Yu et al. [9] proposed a continuous finite-time control scheme for rigid robotic manipulators using a new form of terminal sliding modes so that the finite-time reachability to a boundary layer is guaranteed in the presence of perturbation and external disturbance.

The TSM controllers mentioned above depend on a known model of the robotic manipulator, and need to compute an onerous regression matrix of robot functions from the dynamics of each specific robotic manipulator. To overcome this problem, Fuzzy wavelet network [10] and radial basis function neural network [11] were incorporated into the TSM for control of robot manipulators. However, both these methods are based on *discontinuous* control action.

In this paper, we present a new continuous terminal sliding mode control for a class of MIMO nonlinear uncertain systems, while the dynamics of the plant is identified online requiring no prior knowledge about the dynamics of the plant to be controlled and no off-line learning phase. Fuzzy systems are employed to approximate the plant's unknown nonlinear functions and an adaptive law is derived based on Lyapunov stability analysis for online updating the parameters of the model so that closed-loop stability and finite-time convergence of tracking errors and its derivatives can be guaranteed.

2. Conventional TSM

Consider the following MIMO nonlinear second-order systems represented by

$$\text{`}\ddot{\mathbf{x}}(t) = \mathbf{F}(\mathbf{x}, t) + \mathbf{G}(\mathbf{x}, t) \cdot \mathbf{u}(t) + \mathbf{D}(t) \tag{1}$$

where $\mathbf{x} = [x_1, \dot{x}_1, \ldots, x_m, \dot{x}_m]^T$ is a vector of measurable states and $\ddot{\mathbf{x}} = [\ddot{x}_1, \ldots, \ddot{x}_m]^T$ is the second derivative of the vector $[x_1, \ldots, x_m]^T$, $\mathbf{u} = [u_1, \ldots, u_m]^T$ is the control input vector, $\mathbf{D}(t)$ the external disturbances which is unknown but bounded by the known function, i.e., $\|\mathbf{D}(t)\| \leq \bar{\mathbf{D}}$, $\mathbf{F}(\mathbf{x}, t)$ and $\mathbf{G}(\mathbf{x}, t)$ are unknown continuous functions defined as

$$\mathbf{F}(\mathbf{x}, t) = [f_1(\mathbf{x}, t), \ldots, f_m(\mathbf{x}, t)]^T,$$

$$\mathbf{G}(\mathbf{x}, t) = \begin{bmatrix} g_{11}(\mathbf{x}, t) & \cdots & g_{1m}(\mathbf{x}, t) \\ \vdots & & \vdots \\ g_{m1}(\mathbf{x}, t) & \cdots & g_{mm}(\mathbf{x}, t) \end{bmatrix}$$

but they are estimated as known nominal dynamics $\hat{\mathbf{F}}(\mathbf{x})$ and $\hat{\mathbf{G}}(\mathbf{x})$, respectively, with the bounded estimation errors. With uncertainties, the dynamic equation of the system (1) can be modified as

$$\ddot{\mathbf{x}}(t) = \hat{\mathbf{F}}(\mathbf{x}) + \hat{\mathbf{G}}(\mathbf{x}) \cdot \mathbf{u}(t) + \mathbf{W}(\mathbf{x}, t) \tag{2}$$

where $\mathbf{W}(\mathbf{x}, t)$ is the lumped uncertainty. Here the bound of the lumped uncertainty is assumed to be given; that is,

$$\|\mathbf{W}(\mathbf{x}, t)\| < \rho$$

Throughout this paper we make the following assumptions.

Assumption 1. The matrix $\mathbf{G}(\mathbf{x}, t)$ is positive definite, then it exists $\delta_0 > 0$, $\delta_0 \in \mathsf{R}$ such that $\mathbf{G}(\mathbf{x}, t) > \delta_0 \mathbf{I}_{m \times m}$ where $I_{m \times m}$ is an $m \times m$ identity matrix.

Assumption 2. The desired trajectory $x_{d_i}(t)$, $i = 1, \ldots, m$, is a known bounded function of time with bounded known derivatives and $x_{d_i}(t)$ is assumed to be two times differentiable.

Let us define the tracking error as $e_i = x_{d_i} - x_i$, where x_{d_i} is the desired trajectory. In order to obtain the terminal convergence of the tracking errors, the following first-order terminal sliding variable is defined [3]:

$$s_i = \dot{e}_i + \beta e_i^{q/p} \quad i = 1, \ldots, m \tag{3}$$

where $\beta > 0$ is a design constant, p and q are positive odd integers satisfying $p > q$. To ensure that the terminal sliding mode exists on the switching surface, and this switching surface can be reached in finite time, one has to satisfy the η-reachability condition given below [1]:

$$\frac{1}{2}\frac{d}{dt}s_i^2 < -\eta|s_i| \tag{4}$$

where $\eta > 0$ is a constant. A conventional control law that satisfies (4) for system (1) is given by

$$\mathbf{u}(t) = \hat{\mathbf{G}}^{-1}(\mathbf{x})\left(-\hat{\mathbf{F}}(\mathbf{x}) + \beta\frac{q}{p}\mathbf{e}^{q/p-1}\dot{\mathbf{e}} + (\rho + \eta)\mathrm{sgn}(\mathbf{s})\right) \tag{5}$$

where $\mathbf{s} = [s_1(t), \ldots, s_m(t)]^T$, $\mathrm{sgn}(\mathbf{s}) = [\mathrm{sgn}(s_1), \ldots, \mathrm{sgn}(s_m)]^T$, and $\rho > 0$ is the upper bound of uncertainties and disturbances. If $s_i(0) \neq 0$, the system states will reach sliding mode $s_i = 0$ in the finite time t_r, which satisfies

$$t_{r_i} \leq \frac{|s_i(0)|}{\eta} \tag{6}$$

When the sliding mode is reached (i.e., $\mathbf{s} = 0$), the system dynamics is described by the following nonlinear differential equation

$$s_i = \dot{e}_i + \beta e_i^{q/p} = 0 \quad i = 1, \ldots, m \tag{7}$$

The dynamic Eq. (7) has an equilibrium point at $e_i = 0$. This point is a globally finite-time stable attractor. The convergence time for a solution with any given initial condition $x_i(t_{r_i}) = x_{t_{r_i}}$ to this attractor is finite

$$t_{s_i} = \frac{p}{\beta(p - q)}|x_i(t_{r_i})|^{1-q/p}$$

Remark 1. For the case of $e_i < 0$, the fractional power q/p leads to the term $e_i^{q/p} \notin \Re$, and thus $\dot{e}_i \notin \Re$.

Remark 2. In the case of $e_i(t) = 0$ when $\dot{e}_i(t) \neq 0$, a bounded control signal cannot be guaranteed (see (5)), and a singular condition will result.

Remark 3. The control law (5) is discontinuous across the sliding mode surface, thus causing control chattering which involves extremely high control activity, and furthermore, may excite high-frequency dynamics neglected in the course of modeling.

Remark 4. The larger the system uncertainties, the control law (5) produces higher amplitude of chattering. To avoid such a condition, it is necessary to keep the system uncertainties to a low value and thus an accurate model of the plant is required.

3. Adaptive fuzzy continuous TSM control design

A continuous non-singular TSM is considered in the following form as in [9]:

$$s_i(t) = e_i(t) + \beta|\dot{e}_i|^{\gamma}sign(\dot{e}_i) = 0, \quad i = 1, \ldots, m \tag{8}$$

where $\beta > 0$ and $1 < \gamma < 2$. To implement the continuous TSM controller, a fast TSM-type reaching law is defined as

$$\dot{\mathbf{s}}(t) = -\mathbf{K}_1\mathbf{s}(t) - \mathbf{K}_2 sig(\mathbf{s})^p \tag{9}$$

with $\dot{\mathbf{s}} = [\dot{s}_1(t), \ldots, \dot{s}_m(t)]^T$, $\mathbf{K}_1 = diag(k_{11}, \ldots, k_{1m}) > 0$, $\mathbf{K}_2 = diag(k_{21}, \ldots, k_{2m}) > 0$, $0 < p < 1$, $sig(\mathbf{s}) = [sig(s_1), \ldots, sig(s_m)]^T$ and $sig(s_i)^p = |s_i|^p sign(s_i)$. By differentiating (8) with respect to time, we have

$$\dot{\mathbf{s}} = \dot{\mathbf{e}} + \beta\gamma \, diag(|\dot{\mathbf{e}}|^{\gamma-1})\ddot{\mathbf{e}} \tag{10}$$

By virtue of (1), (8) and (9), the equivalent control law can be written as

$$\mathbf{u}_{eq}(t) = \mathbf{G}^{-1}(\mathbf{x}, t)(-\mathbf{F}(\mathbf{x}, t) - \mathbf{D}(t) + \ddot{\mathbf{x}}_d + \beta^{-1}\gamma^{-1}sig(\dot{\mathbf{e}})^{2-\gamma} + \mathbf{K}_1\mathbf{s} + \mathbf{K}_2 sig(\mathbf{s})^p) \tag{11}$$

Due to the fact that system functions $\mathbf{F}(\mathbf{x}, t)$ and $\mathbf{G}(\mathbf{x}, t)$ and external disturbance $\mathbf{D}(t)$ are unknown in practical systems, the control law (11) is usually difficult to be obtained. Here, we use fuzzy logic system to approximate the nonlinear unknown functions and design an online updating law to estimate the system functions by using Lyapunov stability theory to compensate the approximation errors.

3.1. Regular adaptive fuzzy TSM (AFTSM) controller

Based on the universal approximation theorem [13], fuzzy logic systems can be used to approximate the vector functions $\mathbf{F}(\mathbf{x}, t)$, $\mathbf{D}(t)$ and the matrix function $\mathbf{G}(\mathbf{x}, t)$ in (11). Let $\hat{\mathbf{F}}(\mathbf{x}, \theta_f^t)$ and $\hat{\mathbf{G}}(\mathbf{x}, \theta_g^t)$ be the fuzzy approximation of the vector functions $\mathbf{F}(\mathbf{x}, t) + \mathbf{D}(t)$ and the matrix function $\mathbf{G}(\mathbf{x}, t)$ in (11), respectively. So, (11) can be written as

$$\mathbf{u}_{eq}(t) = \hat{\mathbf{G}}^{-1}(\mathbf{x}, \theta_g^t)(-\hat{\mathbf{F}}(\mathbf{x}, \theta_f^t) + \ddot{\mathbf{x}}_d + \beta^{-1}\gamma^{-1}sig(\dot{\mathbf{e}})^{2-\gamma} + \mathbf{K}_1\mathbf{s} + \mathbf{K}_2 sig(\mathbf{s})^p) \tag{12}$$

Since the approximation $\hat{\mathbf{F}}(\mathbf{x}, \theta_f^t)$ and $\hat{\mathbf{G}}(\mathbf{x}, \theta_g^t)$ are generated online by online estimating the parameters θ_f^t and θ_g^t, there is no guarantee that $\hat{\mathbf{G}}(\mathbf{x}, \theta_g^t)$ remains regular during estimating. To solve this problem, we use the regularized inverse of $\hat{\mathbf{G}}(\mathbf{x}, \theta_g^t)$ defined as [12]

$$\hat{\mathbf{G}}^{-1}(\mathbf{x}, \theta_g^t) = \hat{\mathbf{G}}^T(\mathbf{x}, \theta_g^t)[\varepsilon_0\mathbf{I}_m + \hat{\mathbf{G}}(\mathbf{x}, \theta_g^t)\hat{\mathbf{G}}^T(\mathbf{x}, \theta_g^t)]^{-1} \tag{13}$$

where ε_0 is a small positive constant and $\mathbf{I}_m$ is $m \times m$ identity matrix. Substituting (13) into (12) gives

$$\mathbf{u}_{eq}(t) = \hat{\mathbf{G}}^T(\mathbf{x}, \theta_g^t)[\varepsilon_0\mathbf{I}_m + \hat{\mathbf{G}}(\mathbf{x}, \theta_g^t)\hat{\mathbf{G}}^T(\mathbf{x}, \theta_g^t)]^{-1}(-\hat{\mathbf{F}}(\mathbf{x}, \theta_f^t) + \ddot{\mathbf{x}}_d + \beta^{-1}\gamma^{-1}sig(\dot{\mathbf{e}})^{2-\gamma} + \mathbf{K}_1\mathbf{s} + \mathbf{K}_2 sig(\mathbf{s})^p) \tag{14}$$

The regularized inverse (13) is well defined even when $\hat{\mathbf{G}}(\mathbf{x}, \theta_g^t)$ is singular, and, therefore, the control law defined in (14) is always well defined.

3.2. Fuzzy approximator

To estimate the nonlinear functions $\mathbf{F}(\mathbf{x}, t) + \mathbf{D}(t)$ and $\mathbf{G}(\mathbf{x}, t)$, $m(m + 1)$ fuzzy systems are used. The fuzzy IF–THEN rules are employed to perform a mapping from an input vector $\mathbf{x} = [x_1, x_2, \ldots x_n]^T \in \mathsf{R}^n$ to an output $y \in \mathsf{R}$. The rth fuzzy rule is written as

R^r : if x_1 is $A_1^r(x_1)$ and…and x_n is $A_n^r(x_n)$, then y is B^r

where A_i^r and B_i^r are fuzzy sets with membership functions $\mu_{A_i^r}(x_i)$ and $\mu_{B^i}(y)$, respectively, and $\mathbf{x}$ belongs to a compact set. If we use the product-inference rule, singleton fuzzifier, and center-average defuzzifier then the output of fuzzy logic system can be defined as

$$y = \frac{\sum_{i=1}^{n_r} \tilde{y}^i(\prod_{j=1}^{n} \mu_{A_j^i}(x_j))}{\sum_{i=1}^{n_r} (\prod_{j=1}^{n} \mu_{A_j^i}(x_j))} = \theta^T \psi(\mathbf{x}) \tag{15}$$

where n_r is the number of total fuzzy rules, $\tilde{y}^i$ is the point at which $\mu_{B^i}(\tilde{y}^i) = 1$, $\mu_{A_j^i}(x_j)$ is the membership function of the fuzzy variable x_j characterized by Gaussian function, $\boldsymbol{\theta} = [\tilde{y}^1, \tilde{y}^2 \dots, \tilde{y}^{n_r}]^T$ is an adjustable parameter vector, and $\boldsymbol{\psi} = [\psi^1, \psi^2, \dots \psi^{n_r}]^T$ is a fuzzy basis vector, where ψ^i is defined as

$$\psi^i(\mathbf{x}) = \frac{(\prod_{j=1}^n \mu_{A_j^i}(x_j))}{\sum_{i=1}^{n_r} (\prod_{j=1}^n \mu_{A_j^i}(x_j))} \tag{16}$$

So by applying the introduced fuzzy systems in (15), approximation of functions $f_i(\mathbf{x}, t) + d_i(\mathbf{x}, t)$ and $g_{ik}(\mathbf{x}, t)$ can be expressed as follows:

$$\hat{f}_i(\mathbf{x}, \theta_{f_i}^t) = \theta_{f_i}^T \psi_{f_i}(\mathbf{x}), \quad i = 1, \dots, m \tag{17}$$

$$\hat{g}_{ij}(\mathbf{x}, \theta_{g_{ij}}^t) = \theta_{g_{ij}}^T \psi_{g_{ij}}(\mathbf{x}), \quad i, j = 1, \dots, m \tag{18}$$

where $\theta_{f_i}^t$ and $\theta_{g_{ij}}^t$ are adjustable parameter vectors. Optimal parameters $\theta_{f_i}^*$ and $\theta_{g_{ij}}^*$ can be defined such that:

$$\theta_{f_i}^* = \arg \min_{\theta_{f_i}^t} \left\{ \sup_{x \in D_x} |f_i(\mathbf{x}, t) + d_i(\mathbf{x}, t) - \widehat{f}_i(\mathbf{x}, \theta_{f_i}^t)| \right\} \tag{19}$$

$$\theta_{g_{ij}}^* = \arg \min_{\theta_{g_{ij}}^t} \left\{ \sup_{x \in D_x} |g_{ij}(\mathbf{x}, t) - \widehat{g}_{ij}(\mathbf{x}, \theta_{g_{ij}}^t)| \right\} \tag{20}$$

And minimum estimation errors as

$$\varepsilon_f(\mathbf{x}, t) = \mathbf{F}(\mathbf{x}, t) + \mathbf{D}(t) - \mathbf{F}^*(\mathbf{x}, \boldsymbol{\theta}_f^*) \tag{21}$$

$$\varepsilon_g(\mathbf{x}, t) = \mathbf{G}(\mathbf{x}, t) - \mathbf{G}^*(\mathbf{x}, \boldsymbol{\theta}_\mathbf{g}^*) \tag{22}$$

It is assumed that minimum estimation errors are bounded for all $\mathbf{x} \in D_x$:

$$|\varepsilon_{f_{ij}}(\mathbf{x}, t)| \le \bar{\varepsilon}_f, |\varepsilon_{g_{ij}}(\mathbf{x}, t)| \le \bar{\varepsilon}_g, \quad \forall \mathbf{x} \in D_x \tag{23}$$

that $\bar{\varepsilon}_f$ and $\bar{\varepsilon}_g$ are positive constants.

3.3. Adaptive updating laws

To generate the approximations $\hat{\mathbf{F}}(\mathbf{x}, \boldsymbol{\theta}_f^t)$ and $\hat{\mathbf{G}}(\mathbf{x}, \boldsymbol{\theta}_g^t)$ online, adaptive update laws to adjust the parameter vectors in (16) and (17) need to be developed. The update laws are chosen as

$$\dot{\theta}_{f_i}^t = -\eta_{f_i} \beta \gamma |\dot{e}_i|^{\gamma-1} \psi_{f_i}(\mathbf{x}) s_i \tag{24}$$

$$\dot{\theta}_{g_{ij}}^t = -\eta_{g_{ij}} \beta \gamma |\dot{e}_i|^{\gamma-1} \psi_{g_{ij}}(\mathbf{x}) s_i u_{eq_j} \tag{25}$$

where $\eta_{f_i} > 0$ and $\eta_{g_{ij}} > 0$. Also, a corrective controller is defined to guarantee the stability of the closed-loop control system and compensate the approximation errors. A control input is chosen as

$$\mathbf{u}(t) = \mathbf{u}_{eq}(t) + \mathbf{u}_c(t) \tag{26}$$

where $\mathbf{u}_{eq}(t)$ is given in (14), and $\mathbf{u}_c(t)$ is defined as

$$\mathbf{u}_c(t) = \frac{\mathbf{s}|\mathbf{s}^T|(\bar{\varepsilon}_f + \bar{\varepsilon}_g|\mathbf{u}_{eq}| + |\mathbf{u}_0|)}{\delta_0 \|\mathbf{s}\|^2} \tag{27}$$

$$\mathbf{u}_0(t) = [\varepsilon_0 \mathbf{I}_m + \hat{\mathbf{G}}(\mathbf{x}, \boldsymbol{\theta}_g^t)\hat{\mathbf{G}}^T(\mathbf{x}, \boldsymbol{\theta}_g^t)]^{-1}(-\hat{\mathbf{F}}(\mathbf{x}, \boldsymbol{\theta}_f^t) + \ddot{\mathbf{x}}_d + \beta^{-1}\gamma^{-1}sig(\dot{\mathbf{e}})^{2-\gamma} + \mathbf{K}_1\mathbf{s} + \mathbf{K}_2 sig(\mathbf{s})^p) \tag{28}$$

Theorem 1. *For the MIMO nonlinear system* (1) *with nonlinear functions* $\mathbf{F}(\mathbf{x}, t)$, $\mathbf{D}(t)$ *and* $\mathbf{G}(\mathbf{x}, t)$ *which are approximated by* (17) *and* (18), *if Assumptions 1 and 2 are hold, the control input is as* (26), *and adaptation laws are selected as* (24) *and* (25), *then we have*

(i) *All signals in the closed-loop system are bounded,* $\boldsymbol{\theta}_f^t$ *and* $\boldsymbol{\theta}_g^t$ *converge to the* $\boldsymbol{\theta}_f^*$ *and* $\boldsymbol{\theta}_g^*$, *respectively when* $t \to \infty$.

(ii) *If* $\mathbf{F}^*(\mathbf{x}, \boldsymbol{\theta}_f^*) = \hat{\mathbf{F}}(\mathbf{x}, \boldsymbol{\theta}_f^t)$ *and* $\mathbf{G}^*(\mathbf{x}, \boldsymbol{\theta}_g^*) = \hat{\mathbf{G}}(\mathbf{x}, \boldsymbol{\theta}_g^t)$ *then tracking errors and their first derivatives converge to zero in finite time.*

(iii) *If* $\mathbf{F}^*(\mathbf{x}, \boldsymbol{\theta}_f^*) \neq \hat{\mathbf{F}}(\mathbf{x}, \boldsymbol{\theta}_f^t)$ *and* $\mathbf{G}^*(\mathbf{x}, \boldsymbol{\theta}_g^*) \neq \hat{\mathbf{G}}(\mathbf{x}, \boldsymbol{\theta}_g^t)$, *then sliding variable converges to the neighborhood of TSM* $\mathbf{s} = 0$ *as* $\|\mathbf{s}\| \leq \varDelta = \min(\varDelta_1, \varDelta_2)$,

$$\varDelta_1 = \frac{\|\hat{\mathbf{F}}(\mathbf{x}, \boldsymbol{\theta}_f^t) - \mathbf{F}^*(\mathbf{x}, \boldsymbol{\theta}_f^*)\| + \|\hat{\mathbf{G}}(\mathbf{x}, \boldsymbol{\theta}_g^t) - \mathbf{G}^*(\mathbf{x}, \boldsymbol{\theta}_g^*)\| \|\mathbf{u}_{eq}\|}{k_1}$$

$$\varDelta_2 = \left(\frac{\|\hat{\mathbf{F}}(\mathbf{x}, \boldsymbol{\theta}_f^t) - \mathbf{F}^*(\mathbf{x}, \boldsymbol{\theta}_f^*)\| + \|\hat{\mathbf{G}}(\mathbf{x}, \boldsymbol{\theta}_g^t) - \mathbf{G}^*(\mathbf{x}, \boldsymbol{\theta}_g^*)\| \|\mathbf{u}_{eq}\|}{k_2} \right)^{1/p}$$

in finite time, where k_1 *and* k_2 *represent the minimum eigenvalues of* $\mathbf{K}_1$ *and* $\mathbf{K}_2$, *respectively. Furthermore, tracking errors and their first derivatives converge to the regions*

$$\|\mathbf{e}\| \leq 2\varDelta, \quad \|\dot{e}\| \leq \left(\frac{\varDelta}{\beta} \right)^{1/\gamma}$$

in finite time.

Remark 5. If a Lyapunov function can be defined as

$$\dot{V}'(\mathbf{x}) + \alpha V'(\mathbf{x}) + \beta V'^r(\mathbf{x}) \leq 0 \tag{29}$$

where $0 < r < 1, 0 < \alpha$, then the settling time is given by [9]

$$t_s \leq \frac{1}{\alpha(1-r)} \ln \frac{\alpha V^{1-r}(\mathbf{x}_0) + \beta}{\beta} \tag{30}$$

Proof. (**i**) Consider the following Lyapunov function candidate

$$V = \frac{1}{2}\mathbf{s}^T \mathbf{s} + \frac{1}{2} \sum_{i=1}^m \frac{1}{\eta_{f_i}} \tilde{\theta}_{f_i}^T \tilde{\theta}_{f_i} + \frac{1}{2} \sum_{i=1}^m \sum_{j=1}^m \frac{1}{\eta_{g_{ij}}} \tilde{\theta}_{g_{ij}}^T \tilde{\theta}_{g_{ij}} \tag{31}$$

where $\tilde{\theta}_{f_i} = \theta_{f_i}^* - \theta_{f_i}^t, \tilde{\theta}_{g_{ij}} = \theta_{g_{ij}}^* - \theta_{g_{ij}}^t$. The time derivative of V is

$$\dot{V} = \mathbf{s}^T \dot{\mathbf{s}} - \sum_{i=1}^m \frac{1}{\eta_{f_i}} \tilde{\theta}_{f_i}^T \dot{\theta}_{f_i}^t - \sum_{i=1}^m \sum_{j=1}^m \frac{1}{\eta_{g_{ij}}} \tilde{\theta}_{g_{ij}}^T \dot{\theta}_{g_{ij}}^t \tag{32}$$

Substituting (26) into (10), we have

$$\dot{\mathbf{s}} = \dot{\mathbf{e}} + \beta\gamma \, diag(|\dot{\mathbf{e}}|^{\gamma-1})\ddot{\mathbf{x}}_d - \beta\gamma \, diag(|\dot{\mathbf{e}}|^{\gamma-1})(\mathbf{F}(\mathbf{x}, t) + \mathbf{D}(t)) - \beta\gamma \, diag(|\dot{\mathbf{e}}|^{\gamma-1})(\mathbf{G}(\mathbf{x}, t) - \hat{\mathbf{G}}(\mathbf{x}, \boldsymbol{\theta}_g^t))\mathbf{u}_{eq}$$

$$- \beta\gamma \, diag(|\dot{\mathbf{e}}|^{\gamma-1})\hat{\mathbf{G}}(\mathbf{x}, \boldsymbol{\theta}_g^t)\mathbf{u}_{eq} - \beta\gamma \, diag(|\dot{\mathbf{e}}|^{\gamma-1})\mathbf{G}(\mathbf{x}, t)\mathbf{u}_c \tag{33}$$

From (26)–(27) and the fact

$$\hat{\mathbf{G}}(\mathbf{x}, \boldsymbol{\theta}_g^t)\hat{\mathbf{G}}^T(\mathbf{x}, \boldsymbol{\theta}_g^t)[\varepsilon_0 \mathbf{I}_m + \hat{\mathbf{G}}(\mathbf{x}, \boldsymbol{\theta}_g^t)\hat{\mathbf{G}}^T(\mathbf{x}, \boldsymbol{\theta}_g^t)]^{-1} = \mathbf{I}_m - \varepsilon_0[\varepsilon_0 \mathbf{I}_m + \hat{\mathbf{G}}(\mathbf{x}, \boldsymbol{\theta}_g^t)\hat{\mathbf{G}}^T(\mathbf{x}, \boldsymbol{\theta}_g^t)]^{-1},$$

we have

$$\dot{\mathbf{s}} = -\underline{\mathbf{K}}_1 \mathbf{s} - \underline{\mathbf{K}}_2 sig(\mathbf{s})^p - \beta\gamma \, diag(|\dot{\mathbf{e}}|^{\gamma-1})(\mathbf{F}(\mathbf{x}, t) + \mathbf{D}(t) - \hat{\mathbf{F}}(\mathbf{x}, \boldsymbol{\theta}_f^t))$$

$$- \beta\gamma \, diag(|\dot{\mathbf{e}}|^{\gamma-1})(\mathbf{G}(\mathbf{x}, t) - \hat{\mathbf{G}}(\mathbf{x}, \boldsymbol{\theta}_g^t))\mathbf{u}_{eq} + \beta\gamma \, diag(|\dot{\mathbf{e}}|^{\gamma-1})\mathbf{u}_0 - \beta\gamma \, diag(|\dot{\mathbf{e}}|^{\gamma-1})\mathbf{G}(\mathbf{x}, t)\mathbf{u}_c \tag{34}$$

where $\underline{\mathbf{K}}_1 = \beta\gamma \, diag(|\dot{\mathbf{e}}|^{\gamma-1})\mathbf{K}_1$ and $\underline{\mathbf{K}}_2 = \beta\gamma \, diag(|\dot{\mathbf{e}}|^{\gamma-1})\mathbf{K}_2$.

It is evident that (21) and (22) can be written

$$\mathbf{F}(\mathbf{x}, t) + \mathbf{D}(t) - \hat{\mathbf{F}}(\mathbf{x}, \theta_f^t) = \mathbf{F}^*(\mathbf{x}, \theta_f^*) - \hat{\mathbf{F}}(\mathbf{x}, \theta_f^t) + \varepsilon_f(\mathbf{x}) \tag{35}$$

$$\mathbf{G}(\mathbf{x}, t) - \hat{\mathbf{G}}(\mathbf{x}, \theta_g^t) = \mathbf{G}^*(\mathbf{x}, \theta_g^*) - \hat{\mathbf{G}}(\mathbf{x}, \theta_g^t) + \varepsilon_g(\mathbf{x}) \tag{36}$$

Substituting (35) and (36) into (34), we have

$$\begin{aligned}
\dot{\mathbf{s}} = &-\underline{\mathbf{K}}_1\mathbf{s} - \underline{\mathbf{K}}_2 sig(\mathbf{s})^p - \beta\gamma\, diag(|\dot{\mathbf{e}}|^{\gamma-1})(\mathbf{F}^*(\mathbf{x}, \theta_f^*) - \hat{\mathbf{F}}(\mathbf{x}, \theta_f^t)) \\
&-\beta\gamma\, diag(|\dot{\mathbf{e}}|^{\gamma-1})(\mathbf{G}^*(\mathbf{x}, \theta_g^*) - \hat{\mathbf{G}}(\mathbf{x}, \theta_g^t))\mathbf{u}_{eq} + \beta\gamma\, diag(|\dot{\mathbf{e}}|^{\gamma-1})\mathbf{u}_0 \\
&-\beta\gamma\, diag(|\dot{\mathbf{e}}|^{\gamma-1})\mathbf{G}(\mathbf{x}, t)\mathbf{u}_c - \beta\gamma\, diag(|\dot{\mathbf{e}}|^{\gamma-1})\varepsilon_f(\mathbf{x}) - \beta\gamma\, diag(|\dot{\mathbf{e}}|^{\gamma-1})\varepsilon_g(\mathbf{x})\mathbf{u}_{eq}
\end{aligned} \tag{37}$$

Multiplying $\mathbf{s^T}$ to (37) gives

$$\begin{aligned}
\mathbf{s}^T\dot{\mathbf{s}} = &-\mathbf{s}^T\underline{\mathbf{K}}_1\mathbf{s} - \mathbf{s}^T\underline{\mathbf{K}}_2 sig(\mathbf{s})^p - \beta\gamma\sum_{i=1}^m \psi_{f_i}^T\tilde{\theta}_{f_i}|e_i|^{\gamma-1}s_i - \beta\gamma\sum_{i=1}^m\sum_{j=1}^m \psi_{g_{ij}}^T\tilde{\theta}_{g_{ij}}|e_i|^{\gamma-1}s_iu_{eq_j} \\
&+\mathbf{s}^T\beta\gamma\, diag(|\dot{\mathbf{e}}|^{\gamma-1})\mathbf{u}_0 - \mathbf{s}^T\beta\gamma\, diag(|\dot{\mathbf{e}}|^{\gamma-1})\mathbf{G}(\mathbf{x}, t)\mathbf{u}_c \\
&-\mathbf{s}^T\beta\gamma\, diag(|\dot{\mathbf{e}}|^{\gamma-1})\varepsilon_f(\mathbf{x}) - \mathbf{s}^T\beta\gamma\, diag(|\dot{\mathbf{e}}|^{\gamma-1})\varepsilon_g(\mathbf{x})\mathbf{u}_{eq}
\end{aligned} \tag{38}$$

Apply (38) to (32), we have

$$\dot{V} = -\mathbf{s}^T\underline{\mathbf{K}}_1\mathbf{s} - \mathbf{s}^T\underline{\mathbf{K}}_2 sig(\mathbf{s})^p + \dot{V}_1 + \dot{V}_2 \tag{39}$$

where

$$\dot{V}_1 = -\sum_{i=1}^m \tilde{\theta}_{f_i}^T\left(\beta\gamma\psi_{f_i}(\mathbf{x})|e_i|^{\gamma-1}s_i + \frac{1}{\eta_{f_i}}\dot{\theta}_{f_i}^t\right) - \sum_{i=1}^m\sum_{j=1}^m \tilde{\theta}_{g_{ij}}^T\left(\beta\gamma\psi_{g_{ij}}(\mathbf{x})\,|e_i|^{\gamma-1}\,s_iu_{eq_j} + \frac{1}{\eta_{g_{ij}}}\dot{\theta}_{g_{ij}}^t\right) \tag{40}$$

$$\dot{V}_2 = \mathbf{s}^T\beta\gamma\, diag(|\dot{\mathbf{e}}|^{\gamma-1})\mathbf{u}_0 - \mathbf{s}^T\beta\gamma\, diag(|\dot{\mathbf{e}}|^{\gamma-1})\mathbf{G}(\mathbf{x}, t)\mathbf{u}_c - \mathbf{s}^T\beta\gamma\, diag(|\dot{\mathbf{e}}|^{\gamma-1})\varepsilon_f(\mathbf{x}) - \mathbf{s}^T\beta\gamma\, diag(|\dot{\mathbf{e}}|^{\gamma-1})\varepsilon_g(\mathbf{x})\mathbf{u}_{eq} \tag{41}$$

Substituting the parameter adaptation laws (24) and (25) into (40) gives

$$\dot{V}_1 = 0 \tag{42}$$

From Assumption 1, we can write

$$\mathbf{s}^T\mathbf{G}(\mathbf{x}, t)\mathbf{s} > \delta_0\|\mathbf{s}\|^2 \tag{43}$$

By multiplying the both side of (43) with $(|\mathbf{s^T}|(\bar{\varepsilon}_f + \bar{\varepsilon}_g|\mathbf{u}_{eq}| + |\mathbf{u}_0|)/\delta_0\|\mathbf{s}\|^2)$, it yields

$$\mathbf{s}^T\mathbf{G}(\mathbf{x}, t)\mathbf{u}_c > |\mathbf{s}^T|(\bar{\varepsilon}_f + \bar{\varepsilon}_g|\mathbf{u}_{eq}| + |\mathbf{u}_0|) \tag{44}$$

From (41) and (44), it yields

$$\dot{V}_2 < 0, \tag{45}$$

and substituting (45) into (39) shows that

$$\dot{V} < -\mathbf{s}^T\underline{\mathbf{K}}_1\mathbf{s} - \mathbf{s}^T\underline{\mathbf{K}}_2 sig(\mathbf{s})^p < 0 \tag{46}$$

Therefore, all signals in the closed-loop system are bounded and

$$
\begin{cases}
\lim \left(\dfrac{1}{2} \sum_{i=1}^{m} \dfrac{1}{\eta_{f_i}} \tilde{\theta}_{f_i}^T \tilde{\theta}_{f_i} + \dfrac{1}{2} \sum_{i=1}^{m} \sum_{j=1}^{m} \dfrac{1}{\eta_{g_{ij}}} \tilde{\theta}_{g_{ij}}^T \tilde{\theta}_{g_{ij}} \right) = 0 \\
t \to \infty
\end{cases}
$$

so $\boldsymbol{\theta}_f^t$ and $\boldsymbol{\theta}_g^t$ converge to the $\boldsymbol{\theta}_f^*$ and $\boldsymbol{\theta}_g^*$, respectively, when $t \to \infty$.

(ii) For $\mathbf{F}^*(\mathbf{x}, \boldsymbol{\theta}_f^*) = \hat{\mathbf{F}}(\mathbf{x}, \boldsymbol{\theta}_f^t)$ and $\mathbf{G}^*(\mathbf{x}, \boldsymbol{\theta}_g^*) = \hat{\mathbf{G}}(\mathbf{x}, \boldsymbol{\theta}_g^t)$, it follows from (38), (41) and (45) that

$$
\dot{V}' < -\mathbf{s}^T \underline{\mathbf{K}}_1 \mathbf{s} - \mathbf{s}^T \underline{\mathbf{K}}_2 sig(\mathbf{s})^p \tag{47}
$$

where $V' = \frac{1}{2} \mathbf{s}^T \mathbf{s}$. Then from lemma 2 in [9], (47) can be rewritten as

$$
\dot{V}' < -2\underline{k}_1 V' - 2^{(p+1)/2} \underline{k}_2 V'^{(p+1)/2} \tag{48}
$$

where $\underline{k}_1$ and $\underline{k}_2$ represent the minimum eigenvalues of $\underline{\mathbf{K}}_1$ and $\underline{\mathbf{K}}_2$, respectively, and $1/2 < (p+1)/2 < 1$. According to the finite-time stability criterion (29) and (48), the continuous NTSM (8) will be reached in finite time

$$
t_s \le \frac{1}{\underline{k}_2(1-p)} \ln \frac{\underline{k}_1 V^{(1-p)/2} + 2^{(p-1)/2} \underline{k}_2}{2^{(p-1)/2} \underline{k}_2} \tag{49}
$$

Thus, the tracking errors and their first derivatives converge to zero in finite time.

(iii) For $\mathbf{F}^*(\mathbf{x}, \boldsymbol{\theta}_f^*) \neq \hat{\mathbf{F}}(\mathbf{x}, \boldsymbol{\theta}_f^t)$ and $\mathbf{G}^*(\mathbf{x}, \boldsymbol{\theta}_g^*) \neq \hat{\mathbf{G}}(\mathbf{x}, \boldsymbol{\theta}_g^t)$, it follows from (38), (41) and (45) that

$$
\dot{V}' < -\mathbf{s}^T \underline{\mathbf{K}}_1 \mathbf{s} - \mathbf{s}^T \underline{\mathbf{K}}_2 sig(\mathbf{s})^p - \beta\gamma \mathbf{s}^T \, diag(|\dot{\mathbf{e}}|^{\gamma-1})(\mathbf{F}^*(\mathbf{x}, \boldsymbol{\theta}_f^*) - \hat{\mathbf{F}}(\mathbf{x}, \boldsymbol{\theta}_f^t))
$$
$$
- \beta\gamma \mathbf{s}^T \, diag(|\dot{\mathbf{e}}|^{\gamma-1})(\mathbf{G}^*(\mathbf{x}, \boldsymbol{\theta}_g^*) - \hat{\mathbf{G}}(\mathbf{x}, \boldsymbol{\theta}_g^t))\mathbf{u}_{eq} \tag{50}
$$

which can be written into following two forms:

$$
\dot{V}' < -\beta\gamma \mathbf{s}^T \, diag(|\dot{\mathbf{e}}|^{\gamma-1})(\mathbf{K}_2 sig(\mathbf{s})^p + (\mathbf{K}_1 + diag((\mathbf{F}^*(\mathbf{x}, \boldsymbol{\theta}_f^*) - \hat{\mathbf{F}}(\mathbf{x}, \boldsymbol{\theta}_f^t))
$$
$$
+ (\mathbf{G}^*(\mathbf{x}, \boldsymbol{\theta}_g^*) - \hat{\mathbf{G}}(\mathbf{x}, \boldsymbol{\theta}_g^t))\mathbf{u}_{eq}) \times diag^{-1}(\mathbf{s}))\mathbf{s}) \tag{51}
$$

$$
\dot{V}' < -\beta\gamma \mathbf{s}^T \, diag(|\dot{\mathbf{e}}|^{\gamma-1})(\mathbf{K}_1 \mathbf{s} + (\mathbf{K}_2 + diag((\mathbf{F}^*(\mathbf{x}, \boldsymbol{\theta}_f^*) - \hat{\mathbf{F}}(\mathbf{x}, \boldsymbol{\theta}_f^t))
$$
$$
+ (\mathbf{G}^*(\mathbf{x}, \boldsymbol{\theta}_g^*) - \hat{\mathbf{G}}(\mathbf{x}, \boldsymbol{\theta}_g^t))\mathbf{u}_{eq}) \times diag^{-1}(sig(\mathbf{s})^p))sig(\mathbf{s})^p) \tag{52}
$$

If the matrix $\mathbf{K}_1 - diag((\mathbf{F}^*(\mathbf{x}, \boldsymbol{\theta}_f^*) - \hat{\mathbf{F}}(\mathbf{x}, \boldsymbol{\theta}_f^t)) + (\mathbf{G}^*(\mathbf{x}, \boldsymbol{\theta}_g^*) - \hat{\mathbf{G}}(\mathbf{x}, \boldsymbol{\theta}_g^t))\mathbf{u}_{eq}) \times diag^{-1}(\mathbf{s})$ is positive definite, then (51) has the same structure as that of (47), thus finite-time stability is guaranteed. Assume $(\mathbf{F}^*(\mathbf{x}, \boldsymbol{\theta}_f^*) - \hat{\mathbf{F}}(\mathbf{x}, \boldsymbol{\theta}_f^t)) + (\mathbf{G}^*(\mathbf{x}, \boldsymbol{\theta}_g^*) - \hat{\mathbf{G}}(\mathbf{x}, \boldsymbol{\theta}_g^t))\mathbf{u}_{eq} = \mathbf{W} = [W_1, \ldots, W_m]$, then if $k_1 - (|W_i|/|s_i|) > 0$, the region

$$
|s_i| \le \frac{|W_i|}{k_1}
$$

$$
\|\mathbf{s}\| \le \frac{\|\mathbf{F}^*(\mathbf{x}, \boldsymbol{\theta}_f^*) - \hat{\mathbf{F}}(\mathbf{x}, \boldsymbol{\theta}_f^t)\| + \|\mathbf{G}^*(\mathbf{x}, \boldsymbol{\theta}_g^*) - \hat{\mathbf{G}}(\mathbf{x}, \boldsymbol{\theta}_g^t)\| \|\mathbf{u}_{eq}\|}{k_1} = \Delta_1 \tag{53}
$$

can be reached in finite time.

For (52), similar to the analysis of (51) and Lemma2 in [9], the region

$$
|s_i|^p \le \frac{|W_i|}{k_2}
$$

$$
\|\mathbf{s}\| \le \left(\frac{\|\mathbf{F}^*(\mathbf{x}, \boldsymbol{\theta}_f^*) - \hat{\mathbf{F}}(\mathbf{x}, \boldsymbol{\theta}_f^t)\| + \|\mathbf{G}^*(\mathbf{x}, \boldsymbol{\theta}_g^*) - \hat{\mathbf{G}}(\mathbf{x}, \boldsymbol{\theta}_g^t)\| \|\mathbf{u}_{eq}\|}{k_2} \right)^{1/p} = \Delta_2 \tag{54}
$$

can be reached in finite time. By virtue of (53) and (54), the region $\|\mathbf{s}\| \leq \Delta = \min(\Delta_1, \Delta_2)$, can be reached in finite time. Since $\|\mathbf{s}\| \leq \Delta$, it implies that $|s_i| \leq \Delta$ for $i = 1, 2, \ldots, m$, and the terminal sliding surface (8) can be rewritten as

$$e_i(t) + \beta |\dot{e}_i|^\gamma sign(\dot{e}_i) = \phi_i, \quad |\phi_i| \leq \Delta \tag{55}$$

or, equivalently

$$e_i(t) + \left(\beta - \frac{\phi_i}{|\dot{e}_i|^\gamma sign(\dot{e}_i)} \right) |\dot{e}_i|^\gamma sign(\dot{e}_i) = 0 \tag{56}$$

when $\beta - (\phi_i / |\dot{e}_i|^\gamma sign(\dot{e}_i)) > 0$, (56) is kept in the form of TSM. Thus the first derivative of tracking error converges to the region

$$|\dot{e}_i| \leq \left(\frac{\Delta}{\beta} \right)^{1/\gamma} \tag{57}$$

in finite time. It follows from (55) and (57) that the tracking error converges to the region

$$|e_i| \leq \beta |\dot{e}_i|^\gamma + |\phi_i| \leq \Delta + \Delta = 2\Delta \tag{58}$$

in finite time. This completes the proof. $\square$

Remark 6. The terms $sig(\dot{\mathbf{e}})^{2-\gamma}$ and $sig(\mathbf{s})^p$ in control law can be considered as a bridge between the discontinuous control ($\gamma \to 2$ or $p \to 0$) and linear control ($\gamma \to 1$ or $p \to 1$). To achieve finite-time reachability and chattering elimination, the design parameters γ and p should be appropriately chosen such that $1 < \gamma < 2$ and $0 < p < 1$.

Remark 7. According to (53) and (54), the parameters k_1 and k_2 can be chosen large enough to make the boundary Δ small. However, increasing the parameters k_1 and k_2 will increase the level of control input and will cause implementation problem.

Remark 8. From Theorem 1(i) and (53) and (54), it can be seen that the boundary Δ converges to zero asymptotically.

4. Simulation studies

A two-link rigid robotic manipulator is used to evaluate the performance of the proposed adaptive TSM control scheme. The dynamic equation of the robotic manipulator is given by [7]

$$\begin{bmatrix} a_{11}(x_2) & a_{12}(x_2) \\ a_{12}(x_2) & a_{22} \end{bmatrix} \begin{bmatrix} \ddot{x}_1 \\ \ddot{x}_2 \end{bmatrix} + \begin{bmatrix} -b_{12}(x_2)\dot{x}_1^2 - 2b_{12}(x_2)\dot{x}_1\dot{x}_2 \\ b_{12}(x_2)\dot{x}_2^2 \end{bmatrix} + \begin{bmatrix} c_1(x_1, x_2)g \\ c_2(x_1, x_2)g \end{bmatrix} = \begin{bmatrix} u_1 \\ u_2 \end{bmatrix} + \begin{bmatrix} d_1 \\ d_2 \end{bmatrix}$$

where x_1 and x_2 are the joint angles and

$$a_{11}(x_2) = (m_1 + m_2)r_1^2 + m_2 r_2^2 + 2m_2 r_1 r_2 \cos(x_2) + J_1,$$

$$a_{12}(x_2) = m_2 r_2^2 + m_2 r_1 r_2 \cos(x_2),$$

$$a_{22} = m_2 r_2^2 J_2,$$

$$b_{12}(x_2) = m_2 r_1 r_2 \sin(x_2),$$

$$c_1(x_1, x_2) = (m_1 + m_2)r_1 \cos(x_2) + m_2 r_2 \cos(x_1 + x_2),$$

$$c_2(x_1, x_2) = m_2 r_2 \cos(x_1 + x_2).$$

The parameter values are $r_1 = 1 \, \text{m}$, $r_2 = 0.8 \, \text{m}$, $J_1 = 5 \, \text{kg m}$, $J_2 = 5 \, \text{kg m}$, $m_1 = 0.5 \, \text{kg}$ and $m_2 = 1.5 \, \text{kg}$. The desired trajectories of the joints are given by $x_{d1}(t) = 1.25 - 7.5e^{-t} + 7/20e^{-4t}$ and $x_{d2}(t) = 1.25 + e^{-t} - 1/4e^{-4t}$. The initial values of the system are selected as $x_1(0) = 1$, $x_2(0) = 1.5$, $\dot{x}_1(0) = \dot{x}_2(0) = 0$ and the initial values
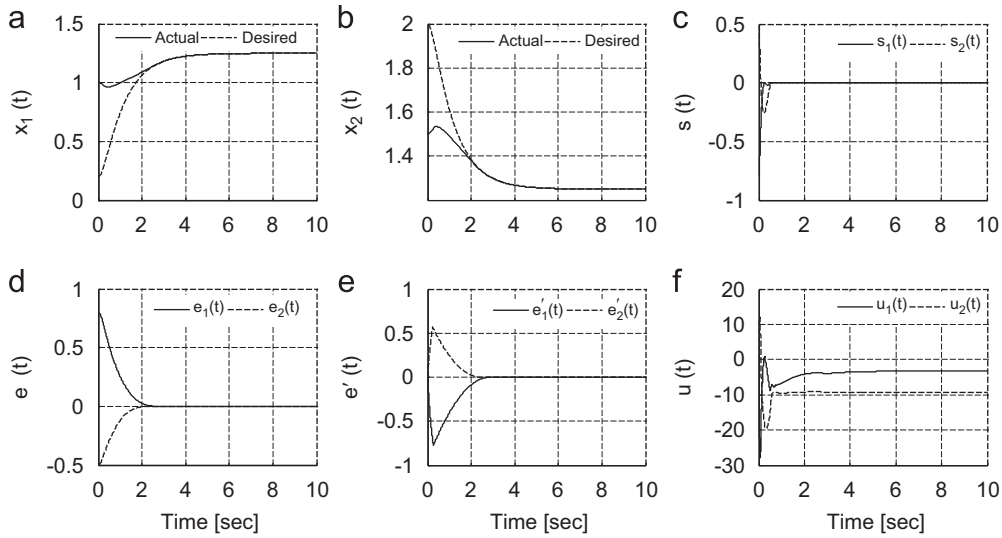
Fig. 1. Control results of a two-link robot manipulator using proposed AFTSM control. (a)–(b) Actual and desired trajectory. (c) TSM. (d) Position tracking error. (e) Velocity tracking error. (f) Control inputs.
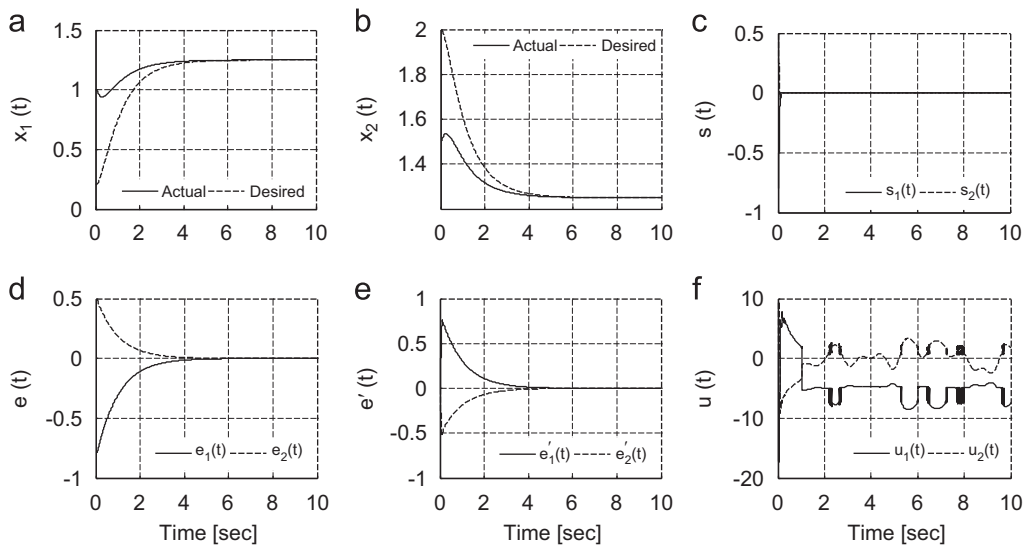

Fig. 2. Control results of a two-link robot manipulator using proposed AFTSM control under time-varying system parameters. (a)–(b) Actual and desired trajectory. (c) TSM. (d) Position tracking error. (e) Velocity tracking error. (f) Control inputs.

of the parameters θ_{f_i} and $\theta_{g_{ij}}$ are set to random values uniformly distributed between [0,1]. The parameters of the controller are chosen heuristically to achieve best controller performance during the first simulation study and used for all simulations as follows:

$$\eta_{f_i} = \eta_{g_{ij}} = 0.45, \quad \varepsilon_0 = 0.1, \quad \bar{\varepsilon}_f = \bar{\varepsilon}_g = 0, \quad \delta_0 = 0.6, \quad \beta = 1,$$

$$\gamma = 1.3, \quad p = 0.1, \quad k_{ij} = 2.5, \quad i, j = 1, 2.$$

The simulation results are shown in Fig. 1. The tracking errors reach boundary layer $\|s\| \leq 6 \times 10^{-4}$ in the finite time $t = 0.617$ s and then converges to $|e_1| \leq 1 \times 10^{-3}$ and $|\dot{e}_1| \leq 1 \times 10^{-3}$ in the finite time $t = 2.604$ and 2.803 s, respectively, and $|e_2| \leq 1 \times 10^{-3}$ and $|\dot{e}_2| \leq 1 \times 10^{-3}$ in the finite time $t = 2.186$ and 2.397 s. It is observed that the
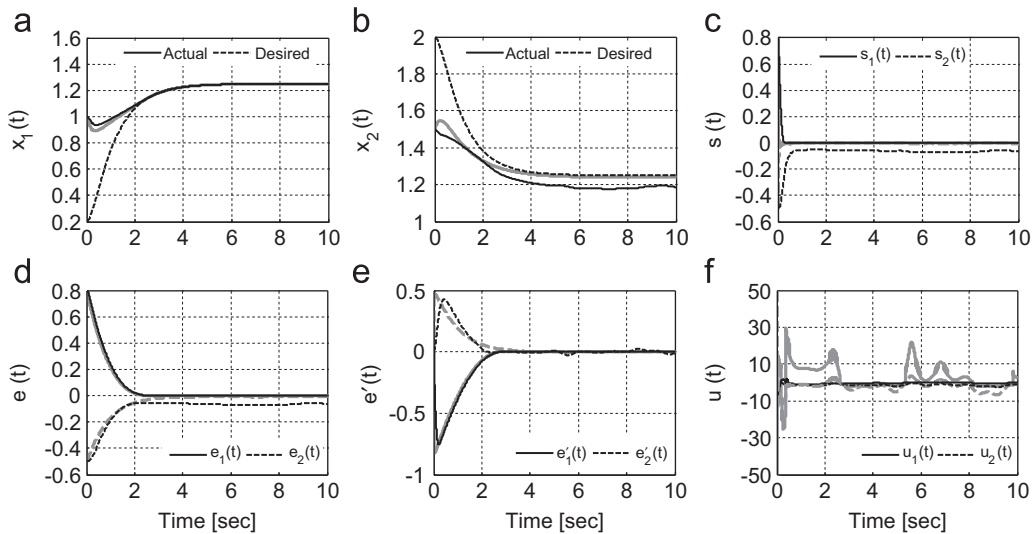
Fig. 3. Control results of a two-link robot manipulator using continuous TSM control [9] under time-varying system parameters for two different values of $k_{ij} = 2.5$ (black) and $k_{ij} = 6$ (gray). (a)–(b) Actual and desired trajectory. (c) TSM. (d) Position tracking error. (e) Velocity tracking error. (f) Control inputs. (For interpretation of the references to color in this figure legend, the reader is referred to the web version of this article.)

control inputs are continuous and chattering-free. This favorable performance was obtained without the requirement of prior knowledge of the plant to be controlled.

To investigate the performance of the proposed controller under time-varying system parameters, the values of the system parameters were varied randomly over $\pm 5\%$ range about their nominal values during the entire period of simulation (10 s). The random variations (uniform distribution) were generated by filtering random sequences with the Butterworth-type low-pass filter whose cutoff frequency was 1 Hz. With the proposed control strategy, the results of simulation are shown in Fig. 2. It can be clearly seen that the tracking errors reach boundary layer $\|s\| \leq 9 \times 10^{-4}$ in the finite time $t = 0.644$ s and then converges to $|e_1| \leq 1 \times 10^{-3}$ and $|\dot{e}_1| \leq 1 \times 10^{-3}$ in the finite time $t = 6.744$ and 6.207 s, respectively, and $|e_2| \leq 1 \times 10^{-3}$ and $|\dot{e}_2| \leq 1 \times 10^{-3}$ in the finite time $t = 5.713$ and 0.644 s. The results of simulation using the continuous TSM control scheme proposed in [9] are shown in Fig. 3. It is clearly observed that a very poor response occurs for continuous TSM control. Although increasing k_{ij} will make the boundary layer smaller and the convergence faster, but the level of the control input will increase.

Fig. 4 shows the response of the controller to a sudden external disturbance. The results clearly demonstrate the fast disturbance rejection and high-precision tracking of the proposed controller while k_{ij} is selected to have values less than the level of the disturbances.

5. Experimental studies

In this section, we investigate the performance of the proposed strategy for control of movement in paralyzed limbs in paraplegic subjects using functional electrical stimulation (FES). Functional electrical stimulation is a promising technique for restoring movement to paralyzed limbs following spinal cord injury, head injury, stroke, and multiple sclerosis [14–17]. In FES systems, sequences of current pulses excite the intact peripheral axon, which in turn contract paralyzed muscles. By changing the pulse width, pulse amplitude, or the pulse frequency, the level of contraction can be altered to perform a specific task. To provide functional use of the paralyzed limbs, an appropriate electrical stimulation pattern should be delivered to a set of muscles.

A major impediment to stimulating the paralyzed neuromuscular systems and determining the stimulation pattern has been the highly nonlinear, time-varying properties of electrically stimulated muscle, muscle fatigue, spasticity, and day-to-day variations which limit the utility of pre-specified stimulation pattern and open-loop FES control system. To deal with these problems, many control strategies have been developed and tested *for control of movement in a single joint*, including fixed-parameter feedback controller [18,19], adaptive feedback techniques [20–23], fixed-parameter
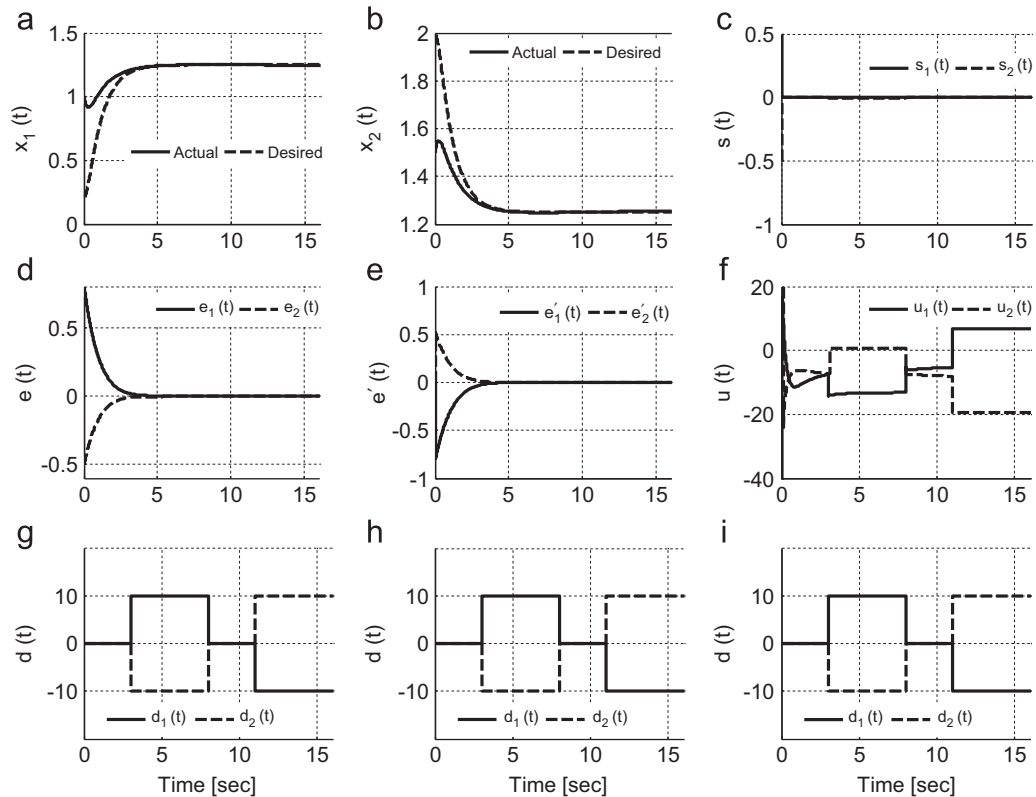
Fig. 4. Control results of external disturbance rejection obtained using proposed AFTSM control. (a)–(b) Actual and desired trajectory. (c) TSM. (d) Position tracking error. (e) Velocity tracking error. (f) Control inputs. (g)–(i) external disturbances.

feedforward [24,25], and adaptive feedforward [25–30]. Moreover, in some studies, the combination of feedforward and feedback control techniques has been proposed [24,25,31] to utilize the advantages of both controller. All these works indicate that tracking quality was improved by the use of the adaptive control law compared to the non-adaptive one. An adaptive control, by online tuning the parameters (of either the plant or the controller—corresponding to the indirect, or direct adaptive control), can deal with uncertainties, but generally, suffers from the disadvantage of being able to achieve only *asymptotical* convergence of the tracking error to zero. Several issues, such as transient performance, unmodeled dynamics, disturbance, the amount of off-line training, the tradeoff between the persistent excitation of signals for correct identification and the steady system response for control performance, the model convergence and system stability issues in real applications and nonlinearity in parameters, often complicate the adaptive approach [32–35].

To overcome these problems, we have already proposed a method which is based on SMC for control of movement in *a single joint* [36,37]. Moreover, the method requires off-line identification of the muscle-joint dynamics, which implies a fundamental limit on its application to FES. In the current study, we employ the adaptive TSMC for control of movement in a multi-joint limb while the controller requires no off-line training phase.

5.1. Experimental procedure

The experiments were conducted on two thoracic-level complete spinal cord injury subjects with injury at T7 and T12 levels using an eight-channel computer-based closed-loop FES system [38]. The subject was seated on a bench with his hip flexed at approximately 90° while the shank was allowed to swing freely and the ankle to plantarflexing and dorsiflexing (Fig. 5). The quadriceps muscle was stimulated using adhesive surface elliptical electrodes (5 × 10 cm GymnaUniphy electrodes, COMEPA Industries, Belgium) that were placed just proximally over the estimated motor
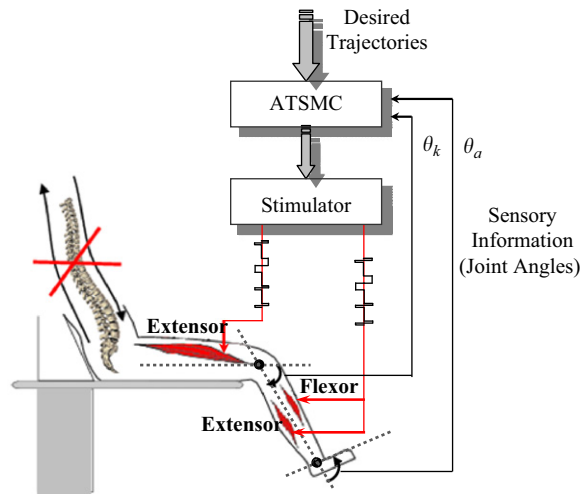
Fig. 5. Experimental setup.

point of rectus femoris and the approximately 4-cm proximal of the patella. The tibialis anterior and calf muscles were stimulated using adhesive surface elliptical electrodes (5×10 cm GymnaUniphy electrodes, COMEPA Industries, Belgium). It should be noted that the gastrocnemius is the most superficial muscle of the calf and is a biarticular muscle that spans both the knee and ankle joints. Pulsewidth modulation (from 0 to 700 μs) with balanced bipolar stimulation pulses, at a constant frequency (25 Hz) and constant amplitude was used. The controller adjusted the pulsewidths and the pulsewidths with negative value were set to zero for control of the quadriceps muscle. For control of the ankle movement, the pulsewidths with positive value were applied to the dorsiflexor and the pulsewidths with negative value to the plantarflexor muscles.

Inertial motion tracking sensors (MTx Motion Tracker, Xsens Technologies, The Netherlands) were used to measure the angle of joints. The computer-based closed-loop FES system uses Matlab Simulink (The Mathworks, R2007b), Real-Time Workshop, and Real-Time Windows Target under Windows 2000/XP for online data acquisition, processing, and controlling. The proposed control strategy was implemented by S-functions using C^{++}.

5.2. Experimental results

The reference trajectories of the knee and ankle joint angles were obtained from an experiment with an able-bodied subject during walking. The parameters of the controller were chosen heuristically to achieve the bestcontroller performance during the first session of experiment as follows:

$$\eta_{f_i} = \eta_{g_{ij}} = 0.5, \quad \varepsilon_0 = 0.1, \quad \bar{\varepsilon}_f = \bar{\varepsilon}_g = 0, \quad \delta_0 = 1, \quad \beta = 1.1, \quad \gamma = 1.15, \quad p = 0.23,$$

$$k_{ij} = 11 \text{ (for subject RR)}, \quad k_{ij} = 13 \text{ (for subject MS)}, \quad i, j = 1, 2.$$

and then used for subsequent experiments on two subjects on different sessions. The root-mean-square (RMS) error was calculated as a measure of tracking accuracy as follows:

$$\text{RMS} = \sqrt{\frac{1}{T} \sum_{t=1}^{T} (\theta(t) - \theta_d(t))^2}$$

Where θ is the measured joint angle, and θ_d the desired trajectory.

Fig. 6 shows typical results of the knee and ankle joints control using the proposed control strategy for two subjects. Excellent tracking performance with no chattering was achieved using the proposed control strategy. The results also show that the method could adjust the stimulation pattern to compensate the muscle fatigue and the tracking performance remains fairly constant throughout the trial. The shift to higher stimulation levels over the course of session indicates
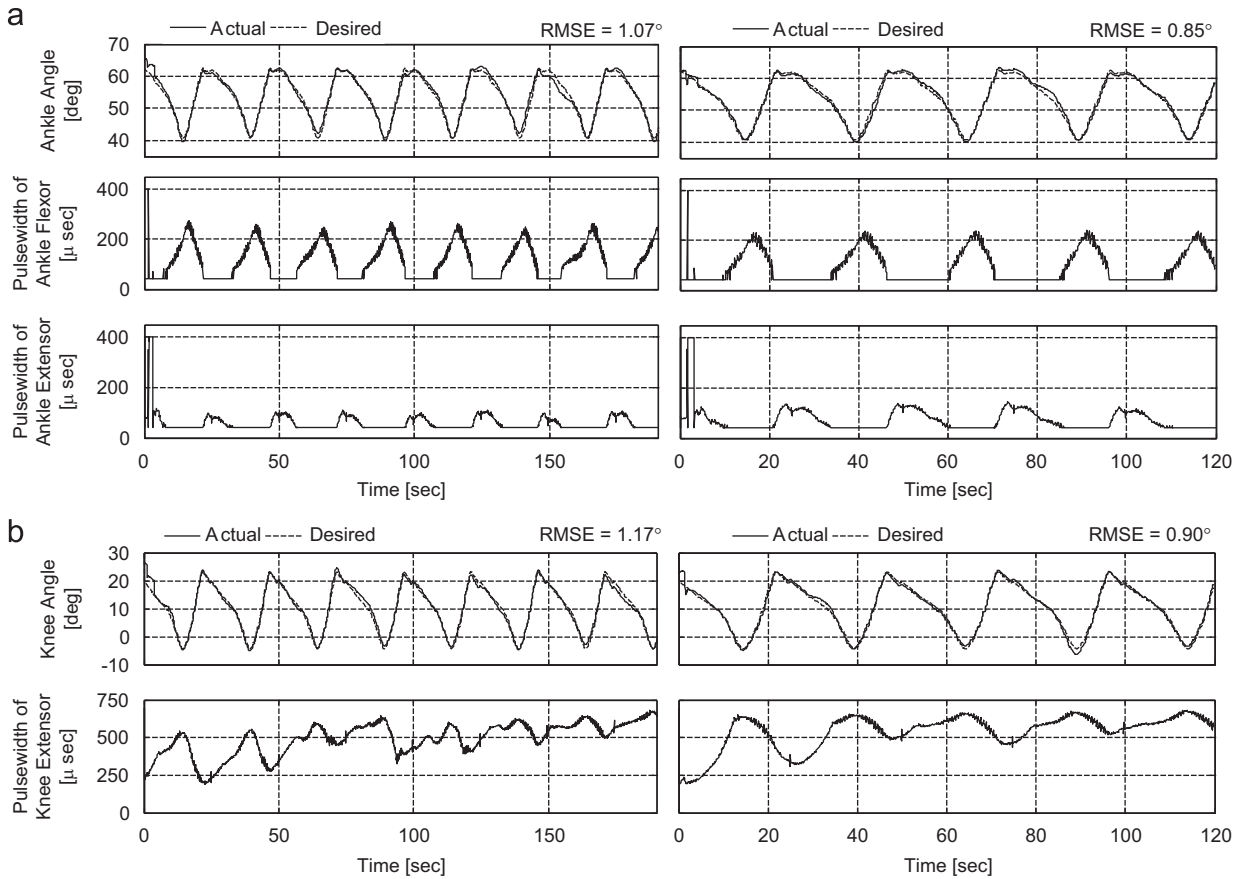
Fig. 6. Typical results of controlling the ankle (a) and knee (b) movements using proposed control strategy on two paraplegic subjects MS (left) and RR (right).

Table 1
Summary of the average daily root-mean-square tracking error ($\pm$ standard deviation) obtained using proposed ATSMC.

Subject	Day	Ankle Joint	Knee Joint
RR	**1**	$2.66° \pm 2.52°$	$1.17° \pm 0.96°$
	2	$2.31° \pm 1.98°$	$1.26° \pm 1.01°$
	3	$1.70° \pm 1.55°$	$1.06° \pm 0.94°$
	Average	$1.69° \pm 0.66°$	
MS	1	$1.75° \pm 1.69°$	$0.98° \pm 0.77°$
	2	$1.54° \pm 1.33°$	$1.14° \pm 0.84°$
	3	$1.07° \pm 1.03°$	$1.16° \pm 1.18°$
	Average	$1.27° \pm 0.30°$	

muscle fatigue (Fig. 6(b)). The most interesting observation is the fast convergence speed of the proposed control strategy. The knee and ankle movement trajectories converge to the desired trajectory after a few seconds.

A summary of results on two subjects over three days (Table 1) indicates that the proposed control strategy is able to achieve and maintain the perfect tracking performance by rapidly adapting the stimulation pattern. Average RMS tracking error is $1.69° \pm 0.66°$ for subject RR and $1.27° \pm 0.30°$ for subject MS. The results demonstrate that the

proposed control strategy provides system dynamics with an invariance property to model uncertainties and day-to-day and subject-to-subject variations.

6. Conclusion

In this paper, an adaptive continuous non-singular sliding mode control has been proposed for a class of nonlinear uncertain systems without relying on a priori knowledge about the dynamics of the system. The proposed controller guarantees not only the bounded-ness of all the signals in the closed-loop system, but also finite-time convergence to the TSM and the equilibrium. The simulation and experimental results confirmed the effectiveness of the proposed adaptive TSM control method. In simulation studies, the ATSM was first applied to control of a two-link rigid robotic manipulator. The results clearly demonstrated the higher-precision control compared with the conventional continuous TSM [9]. Finally, the performance of the controller was evaluated through the control of the ankle and knee movements in paraplegic subjects using functional electrical stimulation. Excellent tracking performance with remarkably fast convergence and with a smooth control action was achieved without requiring off-line identification of the *neuromusculoskeletal* dynamics.

References

[1] J.J.E. Slotine, W. Li, Applied Nonlinear Control, Prentice Hall, New Jersey, 1991.
[2] V. Utkin, J. Guldner, J. Shi, Sliding Mode Control in Electromechanical Systems, Taylor and Francis Ltd, PA, 1999.
[3] M. Zhihong, A.P. Paplinski, H.R. Wu, A robust MIMO terminal sliding mode control scheme for rigid robotic manipulators, IEEE Trans. Autom. Control 39 (1994) 2464–2469.
[4] M. Zhihong, X.H. Yu, Terminal sliding mode control of MIMO linear systems, IEEE Trans. Circuits Syst. I, Fundam. Theory Appl. 44 (1997) 1065–1070.
[5] X.H. Yu, M. Zhihong, Model reference adaptive control systems with terminal sliding modes, Int. J. Control 64 (1996) 1165–1176.
[6] Y. Wu, X. Yu, Z. Man, Terminal sliding mode control design for uncertain dynamic systems, Syst. Control Lett. 34 (1998) 281–287.
[7] Y. Feng, X. Yu, Z. Man, Non-singular terminal sliding mode control of rigid manipulators, Automatica 38 (2002) 2159–2167.
[8] C.W. Tao, J.S. Taur, M.L. Chan, Adaptive fuzzy terminal sliding mode controller for linear systems with mismatched time-varying uncertainties, IEEE Trans. Syst. Man Cybern. B. Cybern. 34 (2004) 255–262.
[9] S. Yu, X. Yu, B. Shirin zadeh, Z. Mand, Continuous finite-time control for robotic manipulators with terminal sliding mode, Automatica 41 (2005) 1957–1964.
[10] C.K. Lin, Nonsingular terminal sliding mode control of robot manipulators using fuzzy wavelet networks, IEEE Trans. Fuzzy Syst. 14 (2006) 849–859.
[11] L. Wang, T. Chai, L. Zhai, Neural-network-based terminal sliding mode control of robotic manipulators including actuator dynamics, IEEE Trans. Ind. Electron. 9 (2009) 3296–3304.
[12] S. Labiod, M.S. Boucherit, T.M. Guerra, Adaptive fuzzy control of a class of MIMO nonlinear systems, Fuzzy Sets Syst. 151 (2005) 59–77.
[13] L.X. Wang, Adaptive Fuzzy Systems and Control: Design and Stability Analysis, Prentice Hall, New Jersey, 1994.
[14] D. Graupe, K.H. Kohn, Functional neuromuscular stimulator for short-distance ambulation by certain thoracic-level spinal-cord-injured paraplegics, Surg. Neurol. 50 (1998) 202–207.
[15] D. Graupe, R. Davis, H. Kordylewski, K. Kohn, Ambulation by traumatic T4–T12 paraplegics using functional neuromuscular stimulation, Crit. Rev. Neurosurg. 8 (1998) 221–231.
[16] D. Popovic, T. Sinkjaer, Control of Movement for the Physically Disabled, Springer Verlag, New York, 2000.
[17] S. Agarwal, R.J. Triolo, R. Kobetic, Long-term user perceptions of an implanted neuroprosthesis for exercise, standing, and transfers after spinal cord injury, J. Rehabil. Res. Dev. 40 (2003) 241–252.
[18] J.J. Abbas, H.J. Chizeck, Feedback control of coronal plane hip angle in paraplegic subjects using functional neuromuscular stimulation, IEEE Trans. Biomed. Eng. 38 (1991) 687–698.
[19] N. Lan, P.E. Crago, H.J. Chizeck, Control of end-point forces of multi-joint limb by functional electrical stimulation, IEEE Trans. Biomed. Eng. 38 (1991) 935–965.
[20] L.A. Bernotas, P.E. Crago, H.J. Chizeck, Adaptive control of electrically stimulated muscle, IEEE Trans. Biomed. Eng. 34 (1987) 140–147.
[21] M.S. Hawell, B.J. Oderkek, C.A. Sacher, G.F. Inbar, The development of a model reference adaptive controller to control the knee joint of paraplegics, IEEE Trans. Automat. Control 36 (1991) 683–691.
[22] J.J. Abbas, H.J. Chizeck, Feedback control methods for task regulation by electrical stimulation of muscle, IEEE Trans. Biomed. Eng. 38 (1991) 1213–1223.
[23] F. Previdi, E. Carpanzano, Design of a gain scheduling controller for knee-joint angle control by using functional electrical stimulation, IEEE Trans. Control Syst. Technol. 11 (2003) 310–324.
[24] G.C. Chang, J.J. Luh, G.D. Liao, J.S. Lai, C.K. Cheng, B.L. Kuo, T.S. Kuo, A neuro-control system for the knee joint position control with quadriceps stimulation, IEEE Trans. Rehabil. Eng. 5 (1997) 2–11.
[25] M. Ferrarin, F. Palazzo, R. Riener, Model based control of FES induced single joint movements, IEEE Trans. Neural Syst. Rehabil. Eng. 9 (2001) 245–257.

[26] J.J. Abbas, H.J. Chizeck, Neural network control of functional neuromuscular stimulation systems: computer simulation studies, IEEE Trans. Biomed. Eng. 42 (1995) 1117–1127.

[27] J.J. Abbas, R.J. Triolo, Experimental evaluation of an adaptive feedforward controller for use in functional neuromuscular stimulation systems, IEEE Trans. Rehabil. Eng. 5 (1997) 12–22.

[28] J. Riess, J.J. Abbas, Adaptive neural control of cyclic movements using functional neuromuscular stimulation, IEEE Trans. Rehabil. Eng. 8 (2000) 42–52.

[29] J. Reiss, J.J. Abbas, Adaptive control of cyclic movements as muscles fatigue using functional neuromuscular stimulation, IEEE Trans. Neural Syst. Rehabil. Eng. 9 (2001) 326–330.

[30] A.R. Mirizarandi, A. Erfanian, H.R. Kobravi, Adaptive inverse control of knee joint position in paraplegic subjects using recurrent neural network, in: 10th Annual Conference of the International Functional Electrical Stimulation Society, Montreal, QC, Canada, 2005.

[31] K. Kurosawa, R. Futami, T. Watanabe, N. Hoshimiya, Joint angle control by FES using a feedback error learning controller, IEEE Trans. Neural Syst. Rehabil. Eng. 13 (2005) 359–371.

[32] P.A. Ioannou, J. Sun, Robust Adaptive Control, Prentice Hall, New Jersey, 1996.

[33] D. Hongliu, S.S. Nair, Learning control design for a class of nonlinear systems, Eng. Appl. Artif. Intell. 11 (1998) 495–505.

[34] T. Zhang, S.S. Ge, C.C. Hang, T.Y. Chai, Adaptive control of first order systems with nonlinear parameterization, IEEE Trans. Automat. Contr. 45 (2000) 1512–1516.

[35] D.E. Miller, A new approach to model reference adaptive control, IEEE Trans. Automat. Control 48 (2003) 743–757.

[36] A. Ajoudani, A. Erfanian, A neuro-sliding mode control with adaptive modeling of uncertainty for control of movement in paralyzed limbs using functional electrical stimulation, IEEE Trans. Biomed. Eng. 56 (2009) 1771–1780.

[37] H.R. Kobravi, A. Erfanian, Decentralized adaptive robust control based on sliding mode and nonlinear compensator for the control of ankle movement using functional electrical stimulation of agonist–antagonist muscles, J. Neural Eng. 6 (2009) 1–10.

[38] H.R. Kobravi, A. Erfanian, A transcutanous computer-based closed-loop motor neuroprosthesis for real-time movement control, in: Proceedings of the Ninth Annual Conference of the International Functional Electrical Stimulation Society, UK, 2004.